Numerical simulation of singular conservation laws and related applications

Guoxian Chen, Magali Ribot

LE STUDIUM
Loire Valley
Institute for Advanced Studies

LE STUDIUM Multidisciplinary Journal

www.lestudium-ias.com

FELLOWSHIP FINAL REPORT

Numerical simulation of singular conservation laws and related applications

Guoxian Chen[1,2,3], Magali Ribot[2]

[1]Computational Science Hubei Key Laboratory, School of Mathematics and Statistics, Wuhan University, Wuhan, 430072, P.R.China
[2]Institut Denis Poisson, Université d'Orléans, Université de Tours, CNRS UMR 7013, BP 6759, F-45067 Orléans Cedex 2, France
[3] LE STUDIUM Institute for Advanced Studies, 45000 Orléans, France

REPORT INFO

Fellow: Professor Guoxian CHEN
From Computational Science Hubei Key Laboratory, School of Mathematics and Statistics, Wuhan University, Wuhan, 430072, P.R.China
Host laboratory in region Centre-Val de Loire: Institut Denis Poisson, Université d'Orléans, Université de Tours, CNRS UMR 7013, BP 6759, F-45067 Orléans Cedex 2, France
Host scientist: Professor Magali RIBOT
Period of residence in region Centre-Val de Loire: January 2018 - January 2019

Keywords :
Balance law, Singularity, Geophysics, Biology, Subcell hydrostatic reconstruction method, Well-balancing, Positivity.

ABSTRACT

We design a scheme for the Euler equations under gravitational fields based on our subcell hydrostatic reconstruction framework.
To give a proper definition of the nonconservative product terms due to the gravitational potential, we first separate the singularity to be an infinitely thin layer, on where the potential is smoothed by defining an intermediate potential without disturbing its monotonicity ; then the physical variables are extended and controlled to be consistent with the Rayleigh-Taylor stability, which contribute the positivity-preserving property to keep the nonnegativity of both gas density and pressure even with vacuum states. By using the hydrostatic equilibrium state variables the well-balanced property is obtained to maintain the steady state even with vacuum fronts. In addition, we proved the full discrete discrete entropy inequality, which preserve the convergence of the solution to the physical solution, with an error term which tends to zero as the mesh size approaches to zero if the potential is Lipschitz continuous. The new scheme is very natural to understand and easy to implement.
The numerical experiments demonstrate the scheme's robustness to resolve the nonlinear waves and vacuum fronts.

1. Introduction

Many interesting physical phenomena, such as atmosphere in weather prediction and climate modeling, as well as astrophysics in solar climate or supernova explosions, are modeled by Euler equations governing the conservation of mass, momentum, and energy. In one dimension, the system can be written as a balance law

$$\frac{\partial}{\partial t}\mathbf{U}+\frac{\partial}{\partial x}\mathbf{F(U)}=-\mathbf{S(U)}\frac{\partial z}{\partial x}\ , \qquad (1.1)$$

where the conservative vector $\mathbf{U}=(\rho,\rho u,E)^{\cdot}$, flux vector $\mathbf{F(U)}=(\rho u,\rho u^2+p,u(E+p))^{\cdot}$, and source term vector $\mathbf{S(U)}=(0,\rho,\rho u)^{\cdot}$.

P1 : The admissible state vectors form a convex invariant set

$$\mathrm{U}=\{\mathbf{U}\in \mathrm{R}^3 \mid \rho>0,\ p>0\}.$$

One often faces the flow near vacuum, for example in the computation of blast waves and high Mach number astrophysical jets. If either density or pressure becomes negative due to numerical oscillations, the calculation will

simply break down. Replacing these negative values with small positive ones violates the mass conservation property and may results in a wrong shock position.

P2 : Another important issue is about the steady states for balance laws, which means that the source term is exactly balanced by the flux gradient,

$$\mathbf{R(U)} := -\frac{\partial}{\partial x}\mathbf{F(U)} - \mathbf{S(U)}\frac{\partial z}{\partial x} = \mathbf{0} \ ,$$

where R is called the residuum. A special steady state, called hydrostatic equilibrium, is when $u = 0$ and

$$\partial_x p = -\rho \partial_x z \ ,$$

which can be solved for polytropic equilibrium

$$\begin{cases} K := p\rho^{-\Gamma} = const \\ \Omega := \begin{cases} T\ln\rho + z, & \Gamma = 1 \\ T\dfrac{\Gamma}{\Gamma - 1} + z, & \Gamma > 1 \end{cases} \\ \quad = const \end{cases}$$

where $\Gamma = 1$ is for the isothermal case where $K = T$; $\Gamma = \gamma$ stands for isentropic case where $K = s$ is the specific entropy.

In many applications, quasi-steady solutions of the balance laws need to be captured on a (practically affordable) coarse grid compared with the deviation from the steady solutions. In such a situation, small physical perturbations of steady states may be submerged by the numerical truncation error which is proportional to the grid size. To prevent such phenomenon, one has to develop a well-balanced scheme which is capable of exactly balancing the flux and source terms to maintain the steady states.

P3 : It is well known that, the system (1.1) admits shock waves solutions. After the work, the system must be supplemented by a entropy inequality

$$\frac{\partial}{\partial t}\tilde{\eta}\mathbf{(U)} + \frac{\partial}{\partial x}\tilde{G}\mathbf{(U)} \le 0 \ ,$$

where the entropy is defined by

$$\tilde{\eta}\mathbf{(U)} = \eta\mathbf{(U)} = \rho f(s) \ ,$$

and its corresponding entropy flux

$$\tilde{G}\mathbf{(U)} = G\mathbf{(U)} = u \cdot \eta(\mathbf{U}) \ ,$$

where $f(\cdot)$ is a smooth non-decreasing function. To make a scheme stable, one needs a discrete version of the entropy inequality.

For the above three properties, the most frequently discussed is P2, i.e. the well-balancing property. This property was pioneerly introduced by Greenberg and Leroux [14] for shallow water equations with topography. The extension to Euler equations under gravitational fields has attracted much attention recently [3,7,8,9,10]. Property P1 is seldom discussed for (1.1). Zhang and Shu extended their positive preserving framework for homogeneous Euler [12] to the inhomogeneous system (1.1) [11]. But their method cannot be applied to preserve the equilibrium. The relaxation Suliciu-type model given by Desveaux et.al. [5] is the only published method preserving P1 and P2 at the same time. But this scheme is not easy to follow. For P3, i.e. entropy inequality, Audusse, et.al. proved the semi-discrete entropy inequalities for shallow water equations [2,13] for their hydrostatic reconstruction (HR) method. We also proved for our recent subcell HR method. In another paper of Audusse et.al. [17], it was proved that when the classical kinetic solver is used, the HR scheme satisfies a fully discrete entropy inequality, but with an error term which is necessary and tends to zero strongly when the mesh size approaches to zero.

We design the subcell HR method [1] to the system (1.1). We will theorically and numerically prove that our new scheme have the above three properties P1,P2 and P3.

2. Experimental details

We use the finite volume scheme to solve (1.1) which updates the approximate cell average

$$\mathbf{U}_i = \frac{1}{\Delta x}\int_{x_{i-1/2}}^{x_{i+1/2}} \mathbf{U}(x,t)dx$$

over cell $[x_{i-1/2},\ x_{i+1/2}]$, with mesh size Δx, from t_n to $t_{n+1}=t_n+\Delta t$ by

$$\mathbf{U}_i^{n+1} = \mathbf{U}_i^n + \Delta t \cdot \mathbf{R}_i$$

where the cell residual is approximated by

$$\Delta x\mathbf{R}_i = \mathbf{R}^+(\mathrm{U}_{i-1}, z_{i-1}, \mathrm{U}_i, z_i) + \mathbf{R}^-(\mathrm{U}_i, z_i, \mathrm{U}_{i+1}, z_{i+1})$$

with the interface residuals $\mathbf{R}^{\pm}$ contributing to the left and right sides of the interface. They are defnied as the limit values

$$\begin{cases} \mathbf{R}^- = \lim\limits_{x\to 0+}\int_{-\grave{o}}^{0} \mathbf{R}(\mathrm{U}^{\grave{o}}, z^{\grave{o}})dx, \\ \mathbf{R}^+ = \lim\limits_{x\to 0+}\int_{0}^{\grave{o}} \mathbf{R}(\mathrm{U}^{\grave{o}}, z^{\grave{o}})dx, \end{cases} \tag{2.1}$$

where $\mathrm{U}^{\grave{o}}, z^{\grave{o}}$ are smoothed data of the following Riemann initial data

$$\begin{pmatrix}\mathbf{U}\\ z\end{pmatrix}(x,0) = \begin{cases} \begin{pmatrix}\mathbf{U}^-\\ z^-\end{pmatrix}, & x<0, \\ \begin{pmatrix}\mathbf{U}^+\\ z^+\end{pmatrix}, & x>0. \end{cases}$$

Algorithm (Subcell HR)

Step 1. Split the cell interfaces into subcells :

$$\{0\} \to [-\grave{o}, 0]\bigcup[0, \grave{o}]\ ;$$

Step 2. Reconstruct the potential on subcells :

Given intermediate potential,

$$z^{\mathring{a}} = \begin{cases} z^{\max}, & \Gamma = 1, \\ \max(\min(z^{\max}, \Omega^-, \Omega^+), \hat{z}^-, \hat{z}^+), & \Gamma \neq 1, \end{cases}$$

where

$$z^{\max} = \max(z^-, z^+)\ , \quad \hat{z} = z - \sqrt{\frac{8}{\gamma(\gamma-1)}}a^2,$$

we set

$$z^{\grave{o}}(x) = \begin{cases} z^{\mathring{a}} + x\dfrac{z^{\mathring{a}} - z^-}{\grave{o}}, & x<0, \\ z^{\mathring{a}} - x\dfrac{z^{\mathring{a}} - z^+}{\grave{o}}, & x>0; \end{cases}$$

Step 3. Reconstruct the state variables on subcells :

K is approximated as a jump function

$$K^{\grave{o}}(x) = \begin{cases} K^-, & x<0, \\ K^+, & x>0. \end{cases}$$

For isothermal case $\Gamma = 1$, Ω is approximated as a jump function

$$\Omega^{\grave{o}}(x) = \begin{cases} \Omega^-, & x<0, \\ \Omega^+, & x>0, \end{cases}$$

thus $\Omega^{\pm,\mathring{a}} := \Omega^{\pm}$; Otherwise

$$\Omega^{\grave{o}}(x) = \begin{cases} \min(\max(\Omega^-, z^{\grave{o}}(x), \Omega^{-,\mathring{a}}), & x<0, \\ \min(\max(\Omega^+, z^{\grave{o}}(x), \Omega^{+,\mathring{a}}), & x>0, \end{cases}$$

with $\Omega^{\pm,\mathring{a}} := \Omega^{\pm} - z^{\pm} + z^{\mathring{a}}$.

3. Results and discussion

Results: Using the above reconstruction, we get intermediate physical variables

$$(\rho,\ u,\ p)^{\pm,\mathring{a}} = (\psi\rho,\ u,\ \psi^{\Gamma}p)^{\pm},$$

and the sub-layer average density

$$\bar{\rho}^{\pm} = \begin{cases} \rho^{\pm}, & z^{\mathring{a}} \le z^{\pm}, \\ -\dfrac{p^{\pm,\mathring{a}} - p^{\pm}}{z^{\mathring{a}} - z^{\pm}}, & z^{\mathring{a}} > z^{\pm}, \end{cases}$$

where the parameters

$$\psi^{\pm} = \begin{cases} \left(\dfrac{\Omega^{\pm,\mathring{a}} - z^{\mathring{a}}}{\Omega^{\pm} - z^{\pm}}\right)^{\frac{1}{\Gamma-1}}, & \Gamma \neq 1, \\ \exp\left(\dfrac{z^{\pm} - z^{\mathring{a}}}{T^{\pm}}\right), & \Gamma = 1. \end{cases}$$

Then we get the interface residuals defined in (2.1) to be

$$\mp\mathbf{R}^{\pm}=\mathbf{F}(\mathbf{U}^{\pm})-F^{\mathring{a}}+(z^{\pm}-z^{\mathring{a}})\bar{\rho}^{\pm}\begin{pmatrix}0\\1\\u^{\pm}\end{pmatrix}$$

where $F^{\mathring{a}}=F(\mathbf{U}^{-,\mathring{a}},\mathbf{U}^{+,\mathring{a}})$ is the numerical flux. Here we use the HLL flux.

Discussions: We directly give the results without giving the proofs. The final results are based on three lemmas at the cell interfaces

Lemma 1(*well-balancing*). Assume that the original interface $\{\mathbf{U}^{-},z^{-},\mathbf{U}^{+},z^{+}\}$ is a hydrostatic equilibrium, then $\mathbf{R}^{\pm}=0.$

Lemma 2(Positivity). Assume that the initial data $\mathbf{U}^{\pm}\in \mathrm{U}\bigcup\{0\}$. Then, Upon the CFL restriction

$$4\lambda\max(|u^{\pm}|+a^{\pm})<1,$$

the updated solution

$$\hat{\mathbf{U}}^{\pm}:=\mathbf{U}^{\pm}+\lambda\mathbf{R}^{\pm}\in \mathrm{U}\bigcup\{0\},$$

Lemma 3(Entropy inequality). Assume that $\mathbf{U}^{\pm}\in \mathrm{U}\bigcup\{0\}$. Then, upon the CFL restriction

$$4\lambda\max(|u^{\pm}|+a^{\pm})<1,$$

The entropy production is upper bounded

$$\eta(\hat{\mathbf{U}}^{\pm})-\eta(\mathbf{U}^{\pm})\pm\lambda(\mathrm{G}(\mathbf{U}^{\pm})-\mathrm{G}^{\mathring{a}})\le c^{\pm}|z^{\mathring{a}}-z^{\pm}|^{\alpha^{\pm}}$$

with

$$\alpha^{\pm}=\begin{cases}2, & z^{\mathring{a}}<\Omega^{\pm},\\ \dfrac{2}{\Gamma-1}, & z^{\mathring{a}}\ge\Omega^{\pm}.\end{cases}$$

Thus we conclude in the following

Theorem. Assume that $\mathbf{U}_i\in \mathrm{U}\bigcup\{0\}$. Then, upon the CFL restriction

$$8\frac{\Delta t}{\Delta x}\lambda\max(|u_i^{\pm}|+a_i^{\pm})<1,$$

we have

(1).The updated solution $\mathbf{U}_i^{n+1}=\mathbf{U}_i$ if both the two interfaces are hydrostatic equilibrium;

(2).The updated solution $\mathbf{U}_i^{n+1}\in \mathrm{U}\bigcup\{0\}$;

(3).The numerical entropy is upper bounded

$$S_i^n:=\frac{\eta(\mathbf{U}_i^{n+1})-\eta(\mathbf{U}_i)}{\Delta t}+\frac{\mathrm{G}^{\mathring{a}}_{i+1/2}-\mathrm{G}^{\mathring{a}}_{i-1/2}}{\Delta x}$$

$$\le\frac{c_i}{\Delta t}\left(|z^{\mathring{a}}_{i-1/2}-z_i|^{\alpha^{+}_{i-1/2}}+|z^{\mathring{a}}_{i+1/2}-z_i|^{\alpha^{-}_{i+1/2}}\right),$$

where

$$\alpha^{\pm}_{i+1/2}=\begin{cases}2, & z^{\mathring{a}}_{i+1/2}<\Omega_{i+1/2\pm1/2},\\ \dfrac{2}{\Gamma-1}, & z^{\mathring{a}}_{i+1/2}\ge\Omega_{i+1/2\pm1/2},\end{cases}$$

4. Numerical Experiments

Example 1. steady state over complex potential.

We consider a complex potential

$$z^{\eth}(x)=\begin{cases}\sin(4\pi x), & x<0.5,\\ \sin(4\pi x)-2, & x>0.5.\end{cases}$$

For isothermal case with $\Gamma=1,$ the initial data are such that $u=0,T=1,\Omega=0.$ The results are displayed in the table which shows that our scheme can preserve the steady state.

# cells	L^1 error of ρ	L^1 error of ρu	L^1 error of E
100	4.28e-15	3.87e-16	5.09e-15
200	5.44e-15	6.85e-16	1.03e-14
400	4.74e-15	1.21e-15	1.37e-14
800	4.57e-15	1.09e-15	3.45e-15
1600	9.39e-15	1.96e-15	2.83e-14
3200	9.37e-15	3.30e-15	3.12e-14

Table 1. The $\mathrm{L}\bar{1}$ errors of the numerical solutions of isothermal equilibrium problem.

For polytropic case with $\Gamma=5/3$. The initial data are such that $u=0,K=1,$

$$\Omega(x)=\begin{cases}\max(0,z(x)) & x<0.5\\ \max(-1.5,z(x)), & x>0.5\end{cases}.$$

The results are represented in the Figure 1. which shows that our scheme can preserve the steady state even there are vacuum fronts.

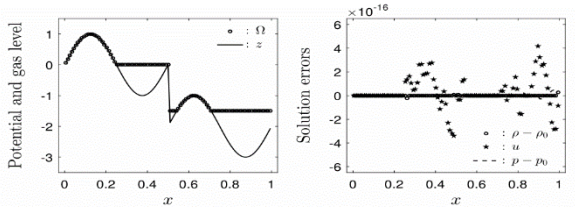

Figure 1. The numerical result of the polytropic equilibrium problem.

Example 2. Perturbation of an steady state.

---Isothermal case. We consider a linear potential $z(x) = x$ over the domain $x \in [0,1]$. The perturbation

$$\delta_p(x) = \eta \exp(-100(x-0.5)^2)$$

is added to the pressure from the steady state with $u = 0, T = 1, \Omega = 0$. The results are shown in Figure 2. We also check the convergence of the numerical solution to the steady state after long time in Figure 3..

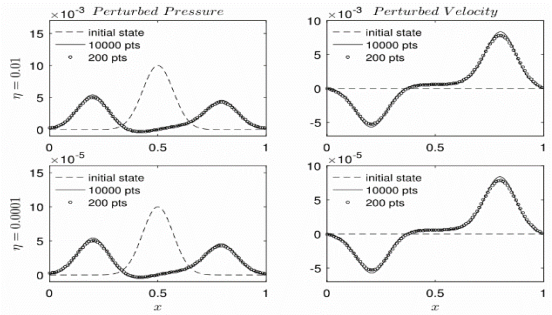

Figure 2. The numerical solution at 0.25 on 200 points of the perturbation from isothermal equilibrium with η=0.01 and η=0.0001.

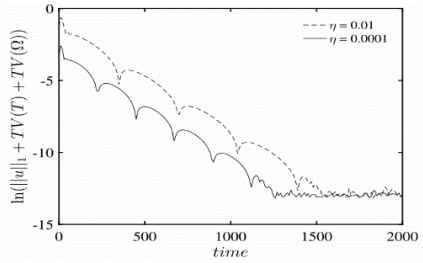

Figure 3. The convergence after lone time.

---Polytropic case. The potential is again a linear function $z(x) = x$ on the domain $[0,3]$. The perturbation

$$u(0,t) = A\sin(4\pi t)$$

with $A = 1.0e-1$ and $A = 1.0e-6$ imposed on the velocity at the left boundary of the equilibria $u = 0, K = 1, \Omega = \max(1/2, z(x))$. The results are shown in Figures 4,5.

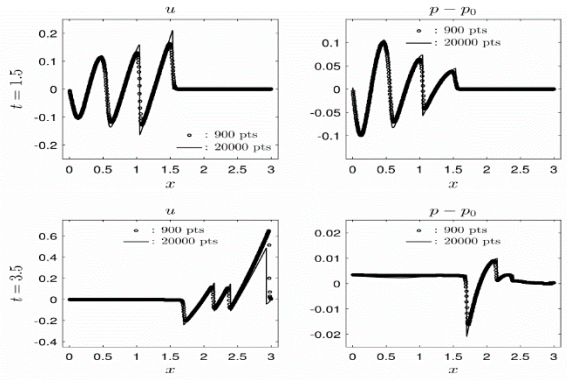

Figure 4. The numerical solution at 1.5 and 3.5 on 900 points of the perturbation from polytropic equilibrium with A=1.0e-1.

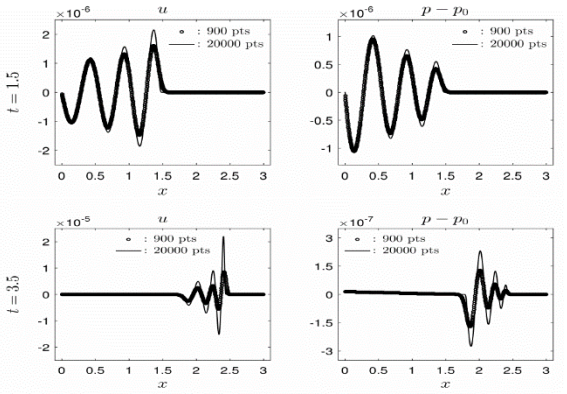

Figure 5. Cont. of Figure 4 with A=1.0e-6.

We also check the convergence to the steady state after long time in Fiugre 6,7.

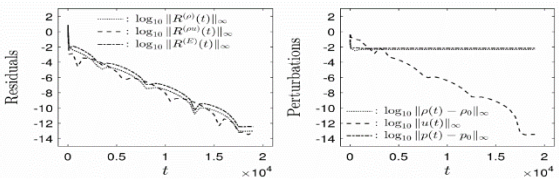

Figure 6. The convergence to the steady state of the numerical solution of perturbation from polytropic equilibrium : A=1.0e-1.

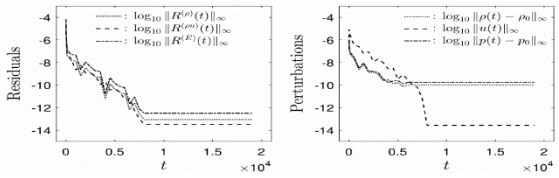

Figure 7. Cont. of Figure 6 with A=1.0e-6.

The results show that the scheme can capture the small perturbations and also that the numerical solution converges to the steady solution after long time simulations.

Example 3. The Riemann problems and entropy production.

We again consider a linear potential on the domain [0,1] . The potential, initial data and output time of four tests are shown in the table 2.

Test	$z(x)$	ρ_L	u_L	p_L	ρ_R	u_R	p_R	t_{final}
1	x	1	0	1	0.125	0	0.1	0.15
2	x	7	-1	0.2	7	1	0.2	0.3
3	x	7	0	0.2	0	0	0	0.4
4	$-x$	7	0	0.2	0	0	0	0.4

Table 2. Four Riemann problems

The numerical results are shown in Figure 8. They prove that the numerical solutions are resolved, and the numerical results produce entropy error which will decrease as the mesh is refined.

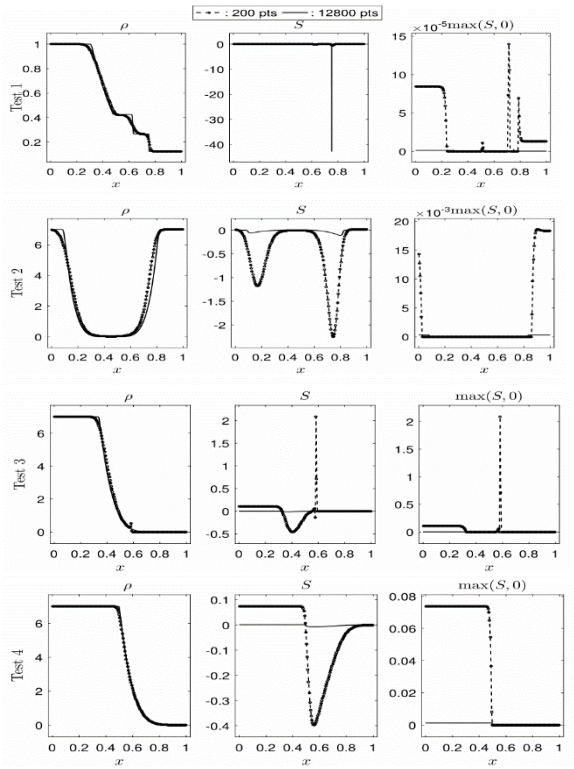

Figure 8. Riemann problems. The densities and entropy productions on 200 points and 12800 points are compared.

5. Conclusion

We designed the subcell HR method to solve the Euler equations under gravitational potential. We proved that our scheme is positive preserving, well-balancing and satisfies the full discrete entropy inequality.

It is done by separating the singularity to be an infinitely thin layer; then smoothing the potential, and extending the physical variables on the layer.

To maintain the steady state numerically, the standard subcell reconstruction is applied on the hydrostatic state variables. To preserve the nonnegativity of both density and pressure, the conservative vectors after extension on the singular layer are controlled. The first step is choosing the local maximum potential for preserving the equilibrium at the interface interfaces.

The well-balaning property is proved. Different from the discussion in the literatures, We consider preserving the general polytropic equilbrium with $\Gamma \geq 1$. We want to mention that the isothermal equilibrium(Γ=1) cannot be connected with the vacuum state, while the polytropic equilibrium with $\Gamma > 1$ can be connected with the vacuum front.

The positivity-preserving property is proved. The invariant domain is chosen different from the literatures. The vacuum state is included, i.e. $U \bigcup \{\mathbf{0}\}$ instead of U is selected for the invariant domain.

We also proved the full discrete entropy inequality with an error term which tends to zero when the mesh size approaches zero if the potential is Lipschitz continuous. It means that the numerical solution will converge to a entropy solution.

The derivation of the new scheme is very natural and easy to implement. The numerical experiments demonstrate that 1) the scheme is robust to resolve the nonlinear waves and vacuum fronts ; 2) the scheme can maintain the general polytropic steady state even with vacuum front ; 3) the entropy error is bounded and will decrease rapidly when the mesh is

refined ; 4) the numerical solution converges to equilibrium after long time.

6. Perspectives of future collaborations with the host laboratory

In the future, we can work together on: (1) designing the scheme for general steady state; (2) the high resolution extension; (3) the applications to high dimensional problems; (4) the applications to other singular problems including the chemotaxis [15] and geophysical flows [16].

7. Articles published in the framework of the fellowship

[1] Guoxian Chen. A Positivity-preserving well-balanced scheme for Euler equations under gravitational fields based on subcell hydrostatic reconstructions, SIAM Journal on Numerical Analysis (2018). submitted for publication.

[2] Guoxian Chen. The subcell hydrostatic reconstruction method for Euler equations under gravitational fields with vacuum front, (2019) working preprint.

8. Acknowledgements

This work was supported by the Le Studium, Loire Valley Institute for Advanced Studies, Orléans & Tours, France under Marie Sklodowska-Curie grand agreement no. 665790, European Commission.

The authors wish to express their warm thanks to Yulong Xing, Francois Bouchut and Sebastian Noelle for many fruitful discussions

9. References

[1] G. Chen and S. Noelle. A new hydrostatic reconstruction scheme based on subcell reconstructions. SIAM Journal on Numerical Analysis, 55(2):758–784, 2017.

[2] F. Bouchut. Nonlinear stability of finite Volume Methods for hyperbolic conservation laws: And Well-Balanced schemes for sources. Springer Science & Business Media, 2004.

[3] P. Chandrashekar and C. Klingenberg. A second order well-balanced finite volume scheme for Euler equations with gravity. SIAM Journal on Scientific Computing, 37(3):B382–B402, 2015.

[4] G. Dal Maso, P. G. Lefloch, and F. Murat. Definition and weak stability of nonconservative products. Journal de mathématiques pures et appliquées, 74(6):483–548, 1995.

[5] V. Desveaux, M. Zenk, C. Berthon, and C. Klingenberg. A well-balanced scheme to capture non-explicit steady states in the euler equations with gravity. International Journal for Numerical Methods in Fluids, 81(2):104–127, 2016.

[6] A. Harten, P. D. Lax, and B. v. Leer. On upstream differencing and Godunov-type schemes for hyperbolic conservation laws. SIAM review, 25(1):35–61, 1983.

[7] R. Käppeli and S. Mishra. Well-balanced schemes for the Euler equations with gravitation. Journal of Computational Physics, 259:199–219, 2014.

[8] G. Li and Y. Xing. High order finite volume WENO schemes for the Euler equations undergravitational fields. Journal of Computational Physics, 316:145–163, 2016.

[9] G. Li and Y. Xing. Well-balanced discontinuous Galerkin methods for the Euler equations under gravitational fields. Journal of Scientific Computing, 67(2):493–513, 2016.

[10] Y. Xing and C.-W. Shu. High order well-balanced WENO scheme for the gas dynamics equations under gravitational fields. Journal of Scientific Computing, 54(2-3):645–662, 2013.

[11] X. Zhang and C.-W. Shu. On positivity-preserving high order discontinuous Galerkin schemes for compressible Euler equations on rectangular meshes. Journal of Computational Physics, 229(23):8918–8934, 2010.

[12] X. Zhang and C.-W. Shu. Positivity-preserving high order discontinuous Galerkin schemes for compressible Euler equations with source terms. Journal of Computational Physics, 230(4):1238–1248, 2011.

[13] E. Audusse, F. Bouchut, M. O. Bristeau, R. Klein, and B. Perthame. A fast and stable well balanced scheme with hydrostatic reconstruction for shallow water flows. SIAM Journal on Scientific Computing, 25(6):2050–2065, 2004.

[14] J. M. Greenberg and A. Y. Leroux. A well-balanced scheme for the numerical processing of source terms in hyperbolic equations. SIAM Journal on Numerical Analysis, 33(1):1–16, 1996.

[15] R. Natalini, M. Ribot, M. warogowska. A well-balanced numerical scheme for a one dimensional quasilinear hyperbolic model of chemotaxis , Commun. Math. Sci. 12 (2014), no.1, 13-39

[16] F. James, P.-Y. Lagrée, M.H. Le, M. Legrand. Towards a new friction model for shallow water equations through an interactive viscous layer, (2018) preprint.

[17] E. Audusse, F. Bouchut, M.-O. Bristeau, and J. Sainte-Marie. Kinetic entropy inequality and hydrostatic reconstruction scheme for the saint-venant system. Mathematics of Computa tion, 85(302):2815–2837, 2016.